Sound & Vibration 2026, 60(4), 3903.
doi: https://doi.org/10.59400/sv3903

Article

Active sound design and sound field equalization for electric vehicles using an order synthesis algorithm and IIR filter-based correction

Xueqing Zhang*, **Jianjiao Deng**, **Jinliang Bi**, **Hao Li**, **Shi Wang**, **Chao Li**, **Chengpeng Zhang**

China First Automobile Group Co., Ltd., Jilin Provincial Key Laboratory of Automotive Vibration and Noise, Changchun 130000, China
* **Corresponding author:** Xueqing Zhang, z18637197509@163.com

CITATION

Zhang X, Deng J, Bi J, et al. Active sound design and sound field equalization for electric vehicles using an order synthesis algorithm and IIR filter-based correction. Sound & Vibration. 2026; 60(4): 3903. https://doi.org/10.59400/sv3903

ARTICLE INFO

Received: 10 January 2026
Revised: 18 April 2026
Accepted: 23 April 2026
Available online: 10 July 2026

COPYRIGHT

Copyright © 2026 Author(s). *Sound & Vibration* is published by Academic Publishing Pte. Ltd. This work is licensed under the Creative Commons Attribution (CC BY) license. https://creativecommons.org/licenses/by/4.0/

Abstract: Active Sound Design (ASD) can enhance the driving experience. At present, the algorithms for synthesizing sound waves have problems of poor robustness and poor sound quality. This study overcomes these problems by introducing a vehicle active sound design order synthesis algorithm that is based on linear interpolation to define a model for the variation of amplitude and frequency with speed. An IIR filter-based sound field equalization and timbre correction method is used to perform frequency-domain correction of four seats in a vehicle to reduce phase interference phenomena. A hardware system based on Field-Programmable Gate Array (FPGA) and Advanced RISC Machines (ARM) was built to configure an electric vehicle sound system. Tone correction, feasibility and stability verification of algorithms, and subjective evaluation of active sound are performed through testing. The Frequency Response Standard Deviation (FRSD) of the four measurement points is used to measure the quality of tone correction, which is improved by 22.9%. The commissioning of the active sound waves based on the hardware system has a frequency response error rate of 5% between the simulated and measured data in the frequency band 0–6,000 Hz. The subjective evaluation of the sound based on four dimensions is used to measure the sound quality and scores 8 points.

Keywords: automotive active sound; order synthesis method; sound field equalization; new energy automobile

1. Introduction

With the global scarcity of resources, new energy automobiles are developing rapidly, but new energy automobiles are quieter to drive and lack acoustic feedback during driving compared to fuel vehicles. The internal engine sound synthesis simulation technology can make up for the regret of the mechanical sound loss due to the low displacement and be used to enhance the sound inside the vehicle to make up for the acoustic feedback and the lack of emotion of the passengers [1]. Emotional voice design not only ensures driving safety but also effectively compensates for the overly quiet operation of new energy vehicles while shaping brand identity [2–4].

Current automotive active sound synthesis methods can be roughly divided into two main categories: granular-based sound synthesis methods and program-based sound synthesis methods. Granular synthesis algorithm requires recording, processing, synthesizing, and replaying engine sound samples from real vehicles, where the frequency and amplitude of the synthesized sounds are correlated with the vehicle's dynamics parameters [5–7], such as different engine revolutions (RPM), throttle loads, and gears. Acoustic particle files must be recorded in an anechoic chamber.

Recorded files shall be categorized and filtered into low-frequency, mid-frequency, and high-frequency groups. Filtered acoustic files require amplitude normalization processing.

In Granular synthesis, short sound particles are first extracted from a track, which usually lasts 10 to 100 milliseconds, and then they are combined according to certain criteria. There are two ways to achieve sound particle file synthesis: the first method organizes the particles into frames, in each of which the parameters of all particles are updated [8]; the second method disperses the particles within a mask that restricts a specific frequency, amplitude, and time region, and the density of the particles within the mask can be varied [9]. Sound particle files must be combined in a way that overlaps and splices them, and there are numerous splicing techniques to choose from, such as harmonic synchronous overlap-and-add [10] (HSOLA), synchronous-overlap-add (SOLA), pitch synchronized overlap-and-add [11] (PSOLA), and waveform similarity overlap-and-add [12] (WSOLA) proposed by Roucos [13], but OLA algorithms cause fundamental frequency breaks in the overlapping part, and even speech distortion.

In addition to particle combination methods, matching must also consider factors such as automotive CAN signals, brand positioning, and styling. Lazaro et al. [14] proposed a model for the interior sound design of an electric vehicle based on the particle synthesis approach. In his model, four particle synthesis parameters are involved: sample source, particle duration, particle envelope, and revolutions per minute range. Xie et al. [15] proposed a vehicle active sound method, which avoids the broadband frequency beat phenomenon due to the mismatch of the sound granular signal parameters, solves the broadband beating problem of the current spliced sound granularity, and ensures the continuity of the synthesized sound. Yu et al. [16] designed a frequency shift and pitch correction sound synthesis algorithm based on an effective variable range fast linear interpolation method, which obtains the Controller Area Network (CAN) signals of an electric vehicle, such as vehicle speed, motor speed, pedal opening, etc., and interpolates the original sound signals with different sampling rates to change the frequency of the sound signals, and then adjusts the amplitude of the sound signals according to different driving states. Chang et al. [17] propose a comprehensive automotive brand sound design process that integrates subjective perception with sound design. Granular synthesis methods are mainly used in video games [18] and some state-of-the-art and high-fidelity driving simulators [19], which are relatively simple to implement and can provide very realistic effects. However, their main drawbacks are that good simulations require a large number of sound samples and the cumbersome process of processing sound files. The particle file interface is prone to “clicky” sounds. The sound design space is severely limited by the timbre of the recorded samples.

The order synthesis method synthesizes sounds based on the physical properties of internal combustion engine sounds [20,21], where each order is a sinusoidal tone of a specific frequency, amplitude, and phase. This method provides real-time acoustic feedback; the synthesis is so simple that it allows for the realization of more complex and vivid sounds with a less complex structure of acoustic parameters [22,23]. There is also a lot of research on order-based sound synthesis algorithms, e.g., Sontacchi et al. [24] proposed the active sound generation (ASG) method to improve the acoustic feedback of a small internal combustion engine or an electric engine, which simulates the number of engine orders and sets each engine order with a parameter set consisting of amplitude, amplitude modulation, and phase modulation related to rotational speed. Zhang et al. [25] designed an active sound generation system (ASGS) and proposed an isochronous in-vehicle sound design methodology that focuses on three dimensions: engine order composition, spectral energy distribution, and sound amplitude enhancement over a range of typical vehicle speeds. Over the next few years, Zhang et al. [26, 27] conducted sound extraction, synthesis, and testing based on the Short-Time Fourier Transform (STFT). He proposed a comprehensive sound design methodology encompassing amplitude, energy, and vehicle speed. Fu et al. [28] designed an active acoustic system to achieve acoustic simulation of electric vehicle acceleration by analyzing the engine order, designing the acoustic signal, and using STFT to reconstruct the signal. Chang et al. [29] built a sound synthesis system using Simulink to simulate the sound of a musical instrument through the study which synthesized the sound using FIR filters. Min et al. [30] proposed an engine sound synthesis method by analyzing the spectral characteristics of internal combustion engine sounds and then synthesized mechanical and fuel sounds using Fourier series. The current research on order synthesis algorithms focuses on analyzing the spectral characteristics of fuel vehicle sound, using sinusoidal signal simulation, which is more based on software simulation to achieve, and has not been carried out in the real vehicle, so the algorithm design sound has limitations. Currently, automotive soundscapes are diverse and no longer centered solely on engine noise. Multi-style sound design better aligns with the evolving demands of active sound design in modern vehicles.

In this article, an order synthesis algorithm has been proposed for active sound design in vehicles, and a system has been built on the whole vehicle and finally played using the vehicle’s audio system, aiming to solve the following aspects:

1. In terms of sound design, the algorithm proposed in this article improves the versatility and flexibility of the algorithmic architecture, which allows the definition of different styles of sound and improves the richness of the sound.
2. In terms of tone reproduction, the tone correction method based on the IIR filter proposed in this article reduces the enhancement and offset of the frequency bands caused by the sound phase interference phenomenon, which facilitates the construction of the whole vehicle with different acoustic performance and ensures the acoustic quality of the sound.
3. Debugging on a real vehicle ensures the stability and robustness of the algorithms and hardware.

The structure of this article is as follows: the first section of the article is an overview of the sound synthesis method for automotive active sound waves; the second section of the article is the definition of the frequency, amplitude, and phase of the order synthesis algorithm; the third section of the article is the equalization of the sound field and timbre correction based on the IIR filter; the fourth section of the article is the sound design based on the order synthesis algorithm; and the fifth section of the article is the construction of the hardware system and the experimental validation.

2. Theory

The Infinite Impulse Response (IIR) filter is characterized by small workload and high computational efficiency, and its design is essentially to find a set of coefficients {b, a} to approximate the required frequency response. Its performance meets the predetermined technical requirements, which can be expressed by an nth-order differential equation [31]:

$$y(n) = -\Sigma a_k y(n-k) + \Sigma b_k x(n-k). \tag{1}$$

Where $y(n)$ and $y(n-k)$ are feedback terms; $x(n-k)$ is the input term; a_k is the output term coefficient; b_k is the input term coefficient.

The block diagram of the second-order discrete all-pass system is shown in **Figure 1**, and the difference equation of this system is:

$$y(n) = \frac{1}{a_0}x(n-2) + \frac{b_1}{a_0}x(n-1) + \frac{b_2}{a_0}x(n) - \frac{a_1}{a_0}y(n-1). \tag{2}$$

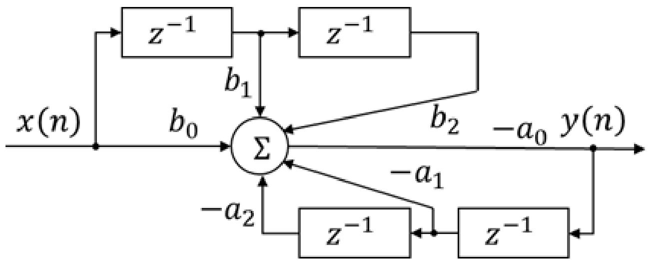

Figure 1. System block diagram of a second-order discrete all-pass system.

The system function is:

$$H(z) = \frac{b_0 + b_1 z^{-1} + b_2 z^{-2}}{a_0 + a_1 z^{-1} + a_2 z^{-2}}. \tag{3}$$

The frequency response of the system is:

$$H\left(e^{j\omega}\right) = \frac{(b_0 + b_2)\cos\omega + b_1 + j(b_0 \sin\omega - b_2 \sin\omega)}{(a_0 + a_2)\cos\omega + a_1 + j(a_0 \sin\omega - a_2 \sin\omega)}. \tag{4}$$

3. Definition of timbre model

Sound is represented by a series of numbers that consist of discrete numerical values or mathematical formulas, while frequency and amplitude are time-varying parameters of these formulas. The order synthesis algorithm is to design the order line. Firstly, the amplitude, frequency, and phase of the order line with time and CAN signals are defined. Secondly, the dynamics model under different working conditions is established. The synthesized data are filtered and equalized. Finally, the sound is played out through the vehicle audio system.

This section mainly defines the timbre of the sound. The amplitude and frequency of the speed of the change in the relationship can be set arbitrarily; you can define a certain speed under the amplitude and frequency changes, which can also be set with the speed of the periodic changes (harmonic). Considering that the amplitude and frequency of sound do not transform linearly with speed, the model in this article is that the amplitude and frequency of each order vary quadratically with speed. When a vehicle accelerates, the frequency and amplitude change faster, and the sound feedback of the tram power sense is more obvious.

3.1. Amplitude definition

In this article, the speed is chosen as the dependent variable of the amplitude, and the amplitude model of sound mainly defines the relationship between amplitude change under different speeds and times of each order. Set different initial amplitudes for various orders at the initial velocity. Then establish a model relating amplitude to velocity and order based on interpolation, or set them individually for different velocities. The specific setting method is shown in **Figure 2**.

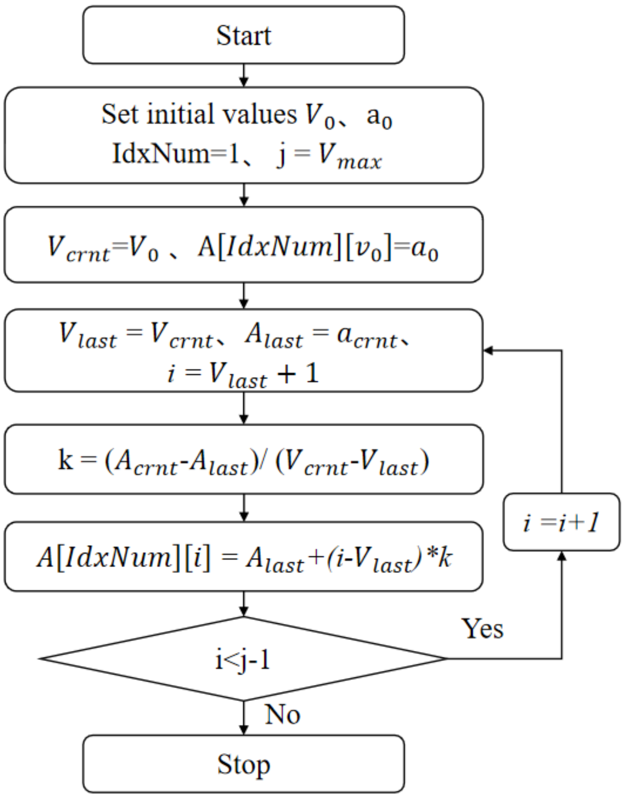

Figure 2. Amplitude definition program flow chart.

3.2. Frequency definition

Frequency is a physical quantity that characterizes the periodicity of a signal [32]. Since pitch reflects the perception of frequency, it should be considered a crucial feature in sound synthesis. Different frequencies produce distinct auditory effects, and the interaction of multiple frequency bands creates rich and diverse sounds. The principle of frequency definition is the same as the definition of amplitude, and the specifics are shown in **Figure 3**.

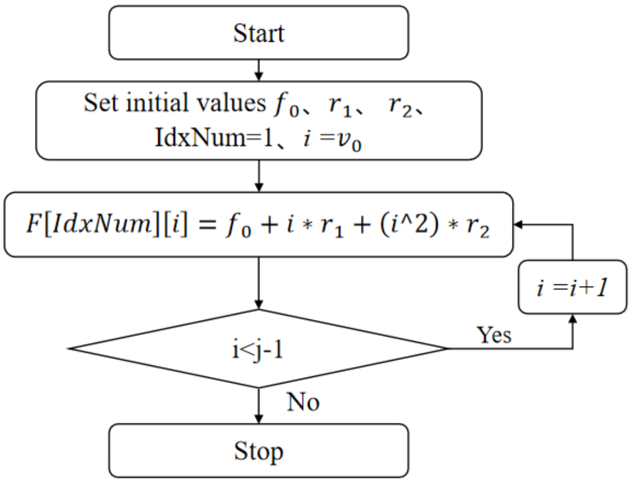

Figure 3. Frequency definition program flow chart.

3.3. Phase definition

The phase of sound can improve sound quality. If a sound has no phase, it will lack authenticity [33]. At present, the research on the influence of sound phase on sound timbre shows that the timbre of a pure tone signal is greatly affected by phase. For example, Plomp [34] proposed that phase has an impact on the timbre of sounds composed of sine or cosine. However, compared with the influence of amplitude, the maximum extent to which phase affects timbre varies from subject to subject (at a 1% level). Automobile simulated sound wave is not a pure tone signal; it is a complex sound signal. The phase of the Automobile simulated sound wave has little effect on timbre. Therefore, this article adopts random phase as the model for sound wave phase.

There is interference between sound phases. To improve the sound quality of sound waves, this article carries out a timbre correction of the sound field in the vehicle in Section 4. First of all, sound wave debugging is based on headphones. After several subjective evaluations, a set of data was initially selected. Then, the initially selected phase data is debugged on the vehicle, and finally the final phase data is determined by multiple real-vehicle subjective evaluations. If the subjective evaluation score reaches 8 points, then the phase model is reasonable. The definition of specific phases is shown in **Figure 4**.

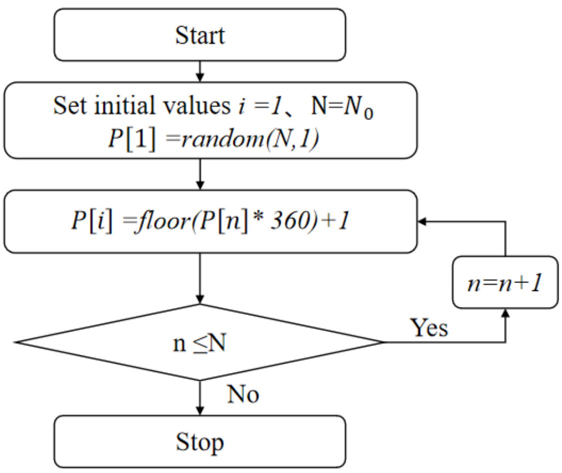

Figure 4. Phase definition program flow chart.

4. Sound field equalization and timbre correction

The purpose of using IIR filters for acoustic field equalization is to adjust the consistency of sound pressure levels and frequencies across four positions within the vehicle. This study enhances in-vehicle sound quality by adjusting the acoustic field at the four seating positions based on an IIR filter, with optimizations applied to both sound pressure levels and frequency response. In debugging, it is necessary to ensure that the frequency response loss of each measuring point is reduced and the frequency response curve is smoother. In the sense of hearing, the sound pressure level and the energy distribution of each frequency at the four measuring points in the car are more consistent. Reducing the influence of the sound field in the car on the sound wave, thereby reducing the difficulty of the sound wave timbre design. These channels include 4 positions: driver, passenger, rear left, and rear right. The difference in the sound pressure level at these 4 positions is improved to less than 3 dB(A). The flowchart is shown in **Figure 5**.

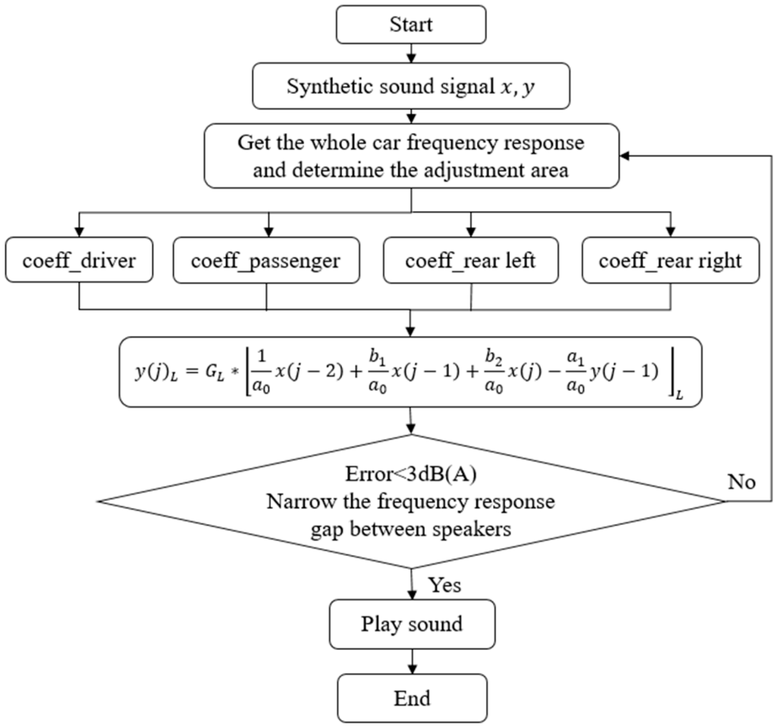

Figure 5. Equalization flowchart (error denotes the sound pressure level error in each speaker).

The test vehicle was stationary in a semi-anechoic chamber, and the white noise was played using four speakers on the car door. The microphones were arranged above each seat, with a total of four microphones for testing the driver, passenger, rear left, and rear right. The microphones were free-field ¼-inch microphones, with the model number B&K4939. The microphone placement on a seat is shown in **Figure 6**. The placement of the microphone and speaker is shown in **Figure 7**. Experimental equipment, speaker parameters, and experimental environment are shown in **Tables 1–3**.

Figure 6. Microphone placement on a seat.

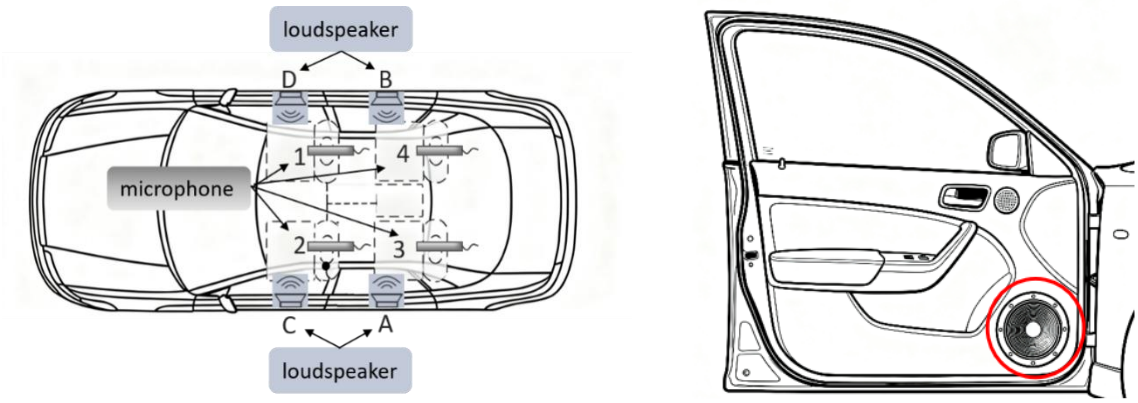

Figure 7. Position of microphones and speakers.

Table 1. Experimental equipment.

Number	Equipment name	Specification and type	Series number	Sensitivity
1	SIEMENS-LMS data acquisition and analysis system	24 channels	25153338	---
2	B&K microphones 4939-A-011	¼-inch free-field	3095435	4 mV/Pa
3	B&K microphones 4939-A-011	¼-inch free-field	3095438	4 mV/Pa
4	B&K microphones 4939-A-011	¼-inch free-field	3070620	4 mV/Pa
5	B&K sound calibrator	type 4231	3028143	±0.2 dB

Table 2. Experiment environment.

Laboratory	Environment temperature (℃)	Environment humidity (RH%)	Background noise (dB(A))
Vehicle semi-anechoic room	25	50	27.8

Table 3. Loudspeaker parameters.

Number	Parameter name	Parameter units	Parameter value
1	Impedance	Ω	4 ± 20%
2	Resonance frequency (F0)	Hz	50 ± 10%
3	Quality Sound (Qts)	/	<0.6
4	Total Harmonic Distortion (THD)	%	<2.5% (50 HZ–4,000 HZ)
5	Characteristic sensitivity	dB	86 ± 1.5(1 m,1 W)
6	Rated power	W	75
7	Rated frequency range	Hz	40–4,000
8	Maximum power	W	110

4.1. Sound balance theory

The signal $y(x_q, t)$ received by the q^{th} microphone is the result of convolving the system response $h_n(x_q, t)$ of the signal *x(t)* emitted by each speaker and the sound wave along the propagation path.

$$y(x_q, t) = \sum\nolimits_{n=1}^{N} x(t) * h_n(x_q, t). \tag{5}$$

Where $q \in [1, Q]$, $n \in [1, N]$; q represents the number of microphones; n represents the number of speakers inside the car that produce sound; $h_n(t)$ represents the transmission signal from the n$^{\text{th}}$ speaker to the q^{th} measurement point; x_q represents the position of the q^{th} microphone.

Performing the Laplace transform on (5) yields:

$$Y(x_q, s) = \sum\nolimits_{n=1}^{N} X(s) * H_n(x_q, s). \tag{6}$$

The frequency response function $H_n(f)$ is:

$$H_n(f) = \sum\nolimits_{n=1}^{N} \frac{Y(x_q, s)}{X(s)}. \tag{7}$$

The amplitude of the frequency response is:

$$|H_n(j\omega)| = \sum\nolimits_{n=1}^{N} \frac{Y(x_q, j\omega)}{X(j\omega)}. \tag{8}$$

The Frequency Response Standard Deviation (FRSD) within a certain frequency band is:

$$\text{FRSD} = \sqrt{\frac{\sum_{i=1}^{M} \left(|H_n(f_i)| - \mu\right)^2}{M}}. \tag{9}$$

Where M is the number of frequency points and μ is the average amplitude of the frequency response.

$$\mu = \frac{\sum_{i=1}^{M} |H_n(f_i)|}{M}. \tag{10}$$

4.2. Sound balance objective results

First of all, white noise is played from the four speakers to obtain the frequency response at the four microphones. The results are shown in **Figure 8**. It can be seen that the differences in sound pressure levels at the four microphone locations are more obvious near the frequencies of 150 Hz, 1,050 Hz, 2,700 Hz, and 3,850 Hz. Around the frequency of 600 Hz, significant energy attenuation occurs at all four positions. The overall trend of attenuation, the attenuation of sound energy, is a reflection of the poor acoustic performance. The sound pressure levels at the 4 microphone positions are shown in **Figure 9**. The difference between the maximum and minimum values is around 8 dB(A), and the difference between the sound pressure levels at the 4 positions in the front and rear rows is large, which means that the sound field is not balanced.

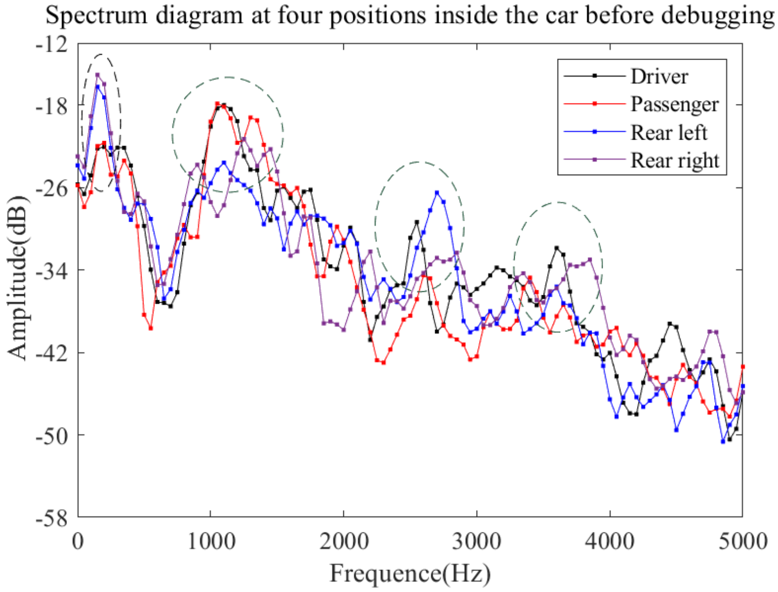

Figure 8. Spectrograms at four locations in the vehicle before commissioning.

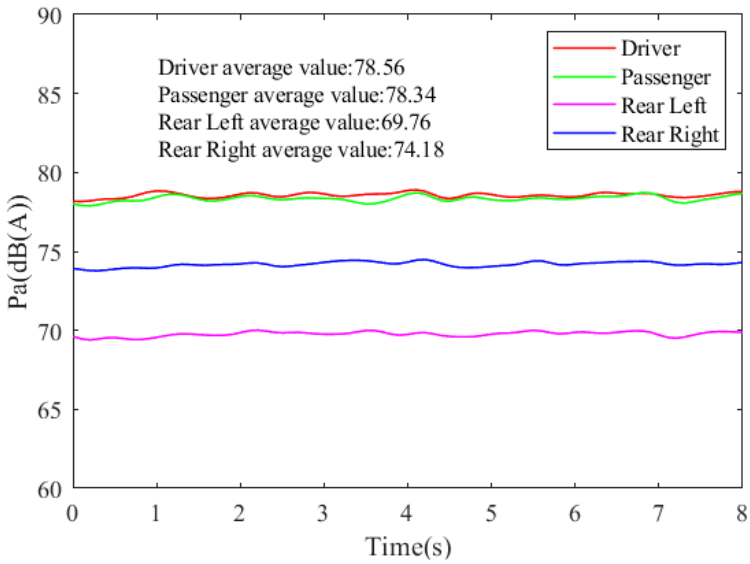

Figure 9. Sound pressure levels at four microphone locations.

Next, the effect of white noise played by the four door speakers on the sound pressure at the four measurement locations in the vehicle is analyzed. Four speakers emit white noise in sequence, and the test results from each speaker to each measuring point are shown in **Figure 10**. According to **Figure 10**, when the center frequency is 150 Hz, it is necessary to reduce the sound pressure at the rear left and rear right. According to **Figure 10a,b**, reducing the white noise played by speakers A and B can lower the sound pressure at the rear left and rear right, as well as the sound pressure of the driver and passenger. However, there is no need to reduce the sound pressure at the driver and passenger. To address this issue, as shown in **Figure 10c,d**, the white noise emitted by loudspeakers C and D has a significant impact on the driver and passenger. Therefore, it is necessary to increase the sound pressure of the white noise played by loudspeakers C and D.

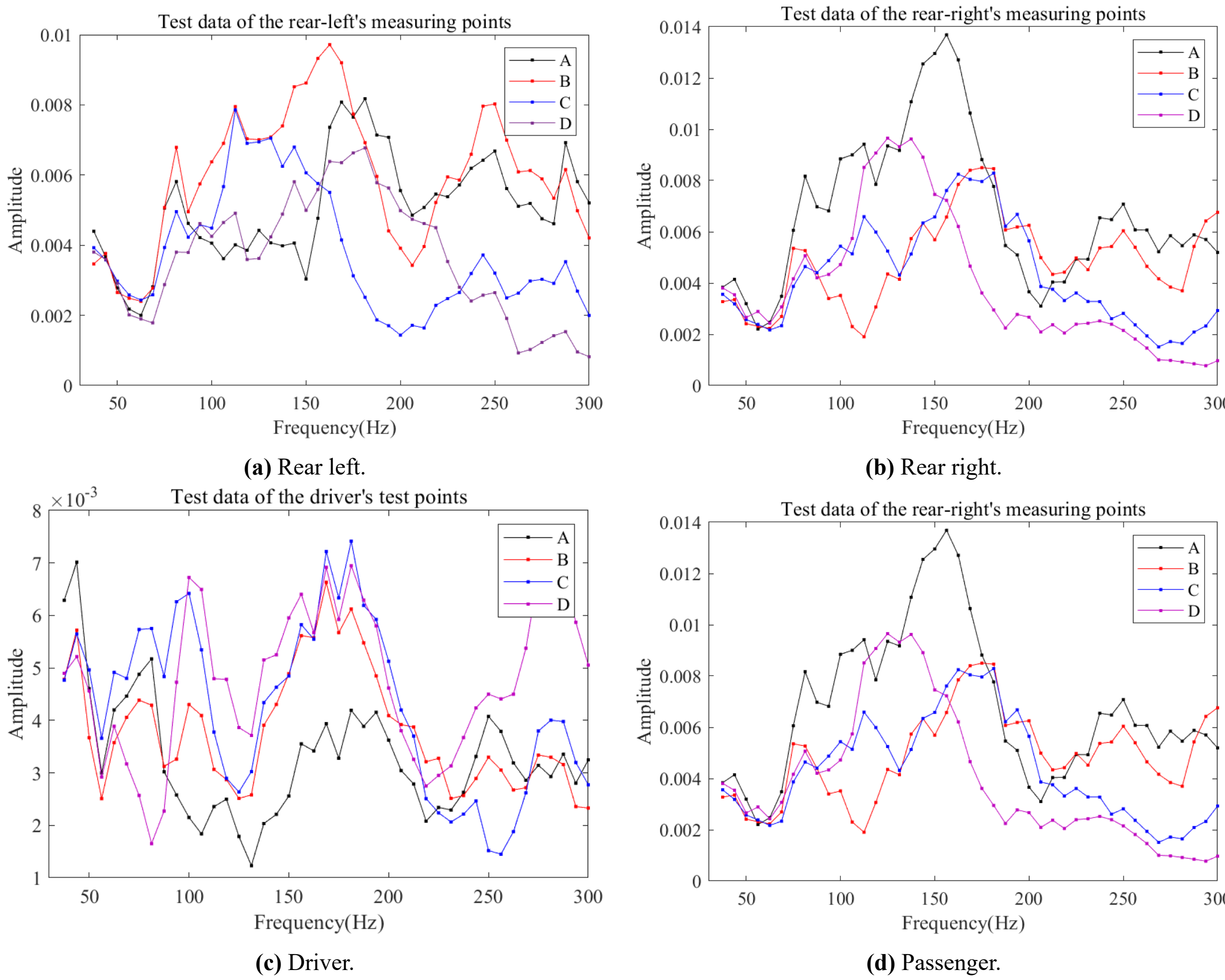

(a) Rear left. **(b)** Rear right. **(c)** Driver. **(d)** Passenger.

Figure 10. Influence of four speakers on sound pressure at four locations in the vehicle.

Use the iirpeak function to increase or suppress the peak value of the output signal of each loudspeaker, set the center frequency f_0, the sampling frequency F_s, the gain, the quality factor Q, the sampling frequency is set to 32,000 Hz, and other parameters. The center frequency is set to 150 Hz, 1,050 Hz, 2,700 Hz, 3,850 Hz in turn; the gain and quality factor Q need to be adjusted according to the actual test situation; the adjustment is repeated until the sound pressure level difference of the sound waves at the four measurement points is within 3 dB(A), and at the same time, certain tone correction is carried out in certain frequency bands. If at the center frequency of 150 Hz, $Q = 2$, gain = 4.5, and the amplitude response is shown in **Appendix A Figure A1**, the transfer function coefficients are obtained.

The IIR filter (Butterworth filter) modifies the sound pressure level, and according to Section 2, the mathematical formula for the IIR second-order digital filter is:

$$H(z) = \frac{b_0 x(k) + b_1 x(k-1) + b_2 x(k-2)}{a_0 y(k) + a_1 y(k-1) + a_2 y(k-2)}. \tag{11}$$

Where $y(k)$ is the value after filtering at the current sample point; $y(k-1)$ is the value after filtering at the previous sample point; $y(k-2)$, $x(k)$ is the value before filtering at the current sample point, $x(k-1)$, $x(k-2)$ and so on.

The Butterworth filter is designed through MATLAB's Filter Designer, with a low-pass filter at 0–300 Hz and a band-pass filter for the rest of the frequency band.

The sampling rate is 32,000 Hz, and the sound design filters for different door speakers are gained or decimated according to different center frequencies (150 Hz, 1,050 Hz, 2,700 Hz, and 3,850 Hz), as shown in **Appendix A Figure A2**.

The designed filter parameters were written into the sound synthesis program and adjusted, and the obtained spectrograms at the four positions in the vehicle are shown in **Figure 11**. At the frequencies of 150 Hz, 1,050 Hz, 2,700 Hz, and 3,850 Hz, the difference between the four positions of the spectrogram is reduced. The sound pressure levels of the four positions are shown in **Figure 12**. The difference between the maximum value and the minimum value is less than 3 dB(A), and the sound field of the four positions of the vehicle is more balanced. It can be seen that after equalization, the interior transfer function curve tends to be flatter. In the sense of hearing, the sound pressure level and the energy distribution of each frequency at the four measuring points in the car are more consistent.

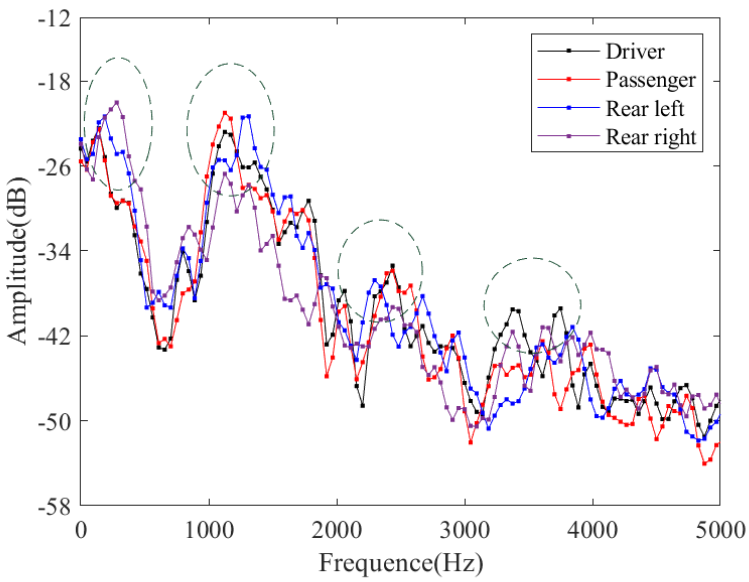

Figure 11. Spectrograms at four locations in the vehicle after commissioning.

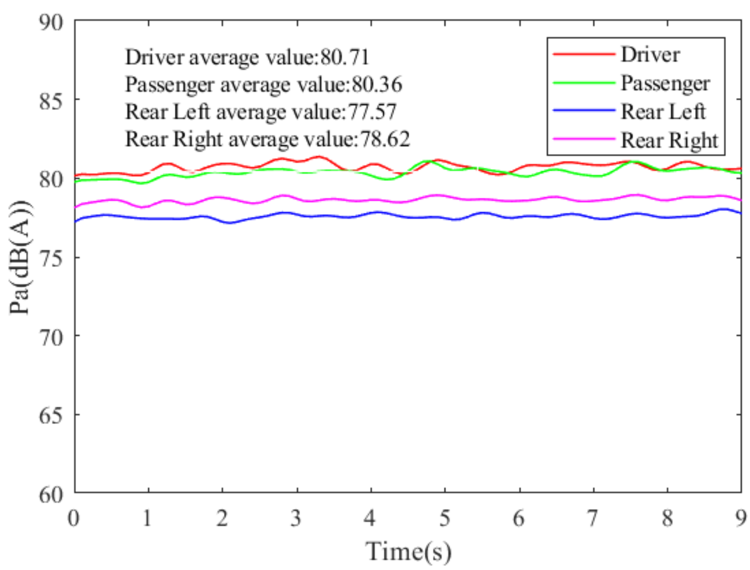

Figure 12. Sound pressure at four positions after commissioning.

The effective frequency range of the speaker used in the test vehicle is 50 Hz–6,000 Hz; therefore, only the FRSD within the effective frequency range of the speakers will be compared. By calculating through formulas (8)–(10), at each frequency point, the FRSD of the four measurement points before and after equalization is averaged, as shown in **Figure 13**. The average FRSD of the four measurement points after balance is 0.17, and the average FRSD after balance is 0.1. Within the effective frequency range of the speaker, the FRSD of the four measuring points improved by 23.5%. At each frequency point, the energy received by the four measuring points is closer. The comparison of the standard deviation of the full frequency response amplitude of four measurement points before and after equalization are shown in **Figure 14**. The FRSD of the full frequency response amplitude of the four measurement points before equalization were 0.21, 0.21, 0.20, and 0.21, respectively. After equalization, they were 0.16, 0.17, 0.15, and 0.16, respectively. The four measurement points improved by 23.8%, 19.0%, 25.0%, and 23.8%, respectively. Regardless of whether it is a full frequency band or a single frequency point, the FRSD after equalization is lower than that before equalization, and the frequency response at the four measurement points is more consistent, resulting in a more balanced sound field inside the car.

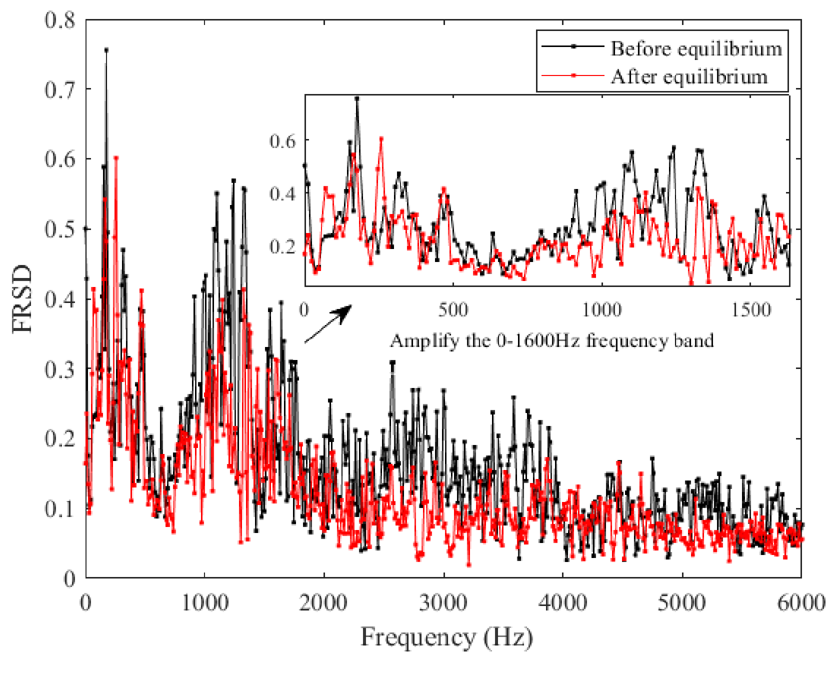

Figure 13. Comparison of the average FRSD of the four measuring points before and after equalization at each frequency point.

4.3. Sound design based on order synthesis algorithms

The sound design is roughly divided into three steps: acquiring the CAN signal, synthesizing the sound, and playing the sound. The flowchart is shown in **Figure 15** below. The ASGS algorithm flowchart is shown in **Figure 16**. The parameter definitions are provided in **Appendix A Table A1**. The order synthesis algorithm is detailed in **Appendix A Algorithm A1**.

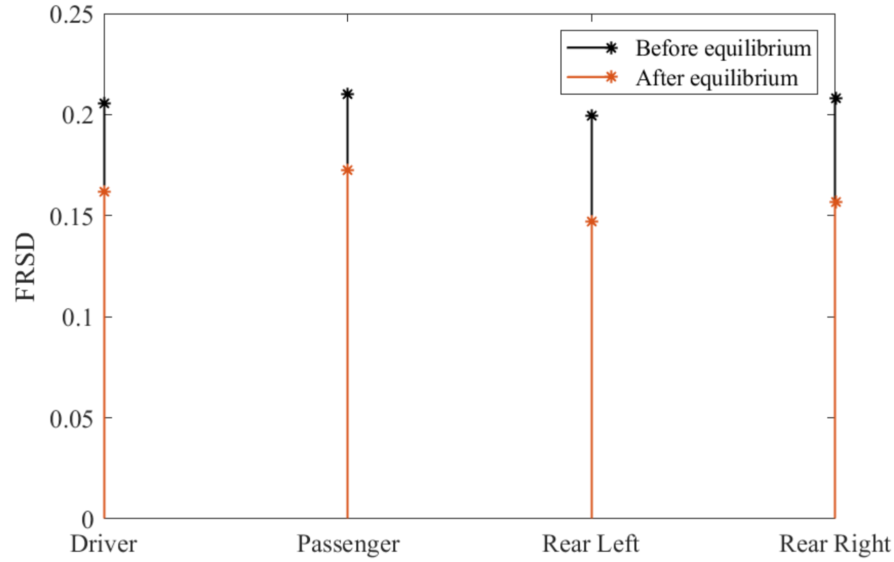

Figure 14. Comparison of FRSD at four measuring points before and after equilibrium across the entire frequency band.

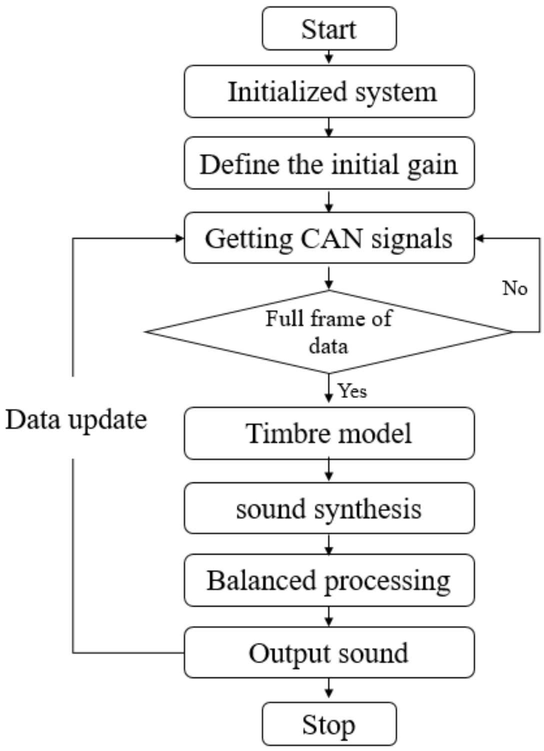

Figure 15. ASGS system functional module flowchart.

First, according to the automotive CAN protocol, the required CAN signals are obtained; this article uses a CAN baud rate of 500 kbps. Then these signals are input into the sound synthesis program, and the synthesized sound is played through the vehicle speakers. The acquired CAN signal curves are shown in **Figure 17**. To facilitate the selection of kinetic parameters, the pedal opening, brake pedal, and vehicle speed are multiplied by certain coefficients, which makes it easy to observe the changes of these signals in the same graph. As shown in **Figure 17**, the torque is negative when the motor absorbs power. The effect of torque must be considered during sound synthesis. After modeling the variation of amplitude and frequency, the variation of sound pressure with the CAN signal (kinetic variation model) considers the effect of torque.

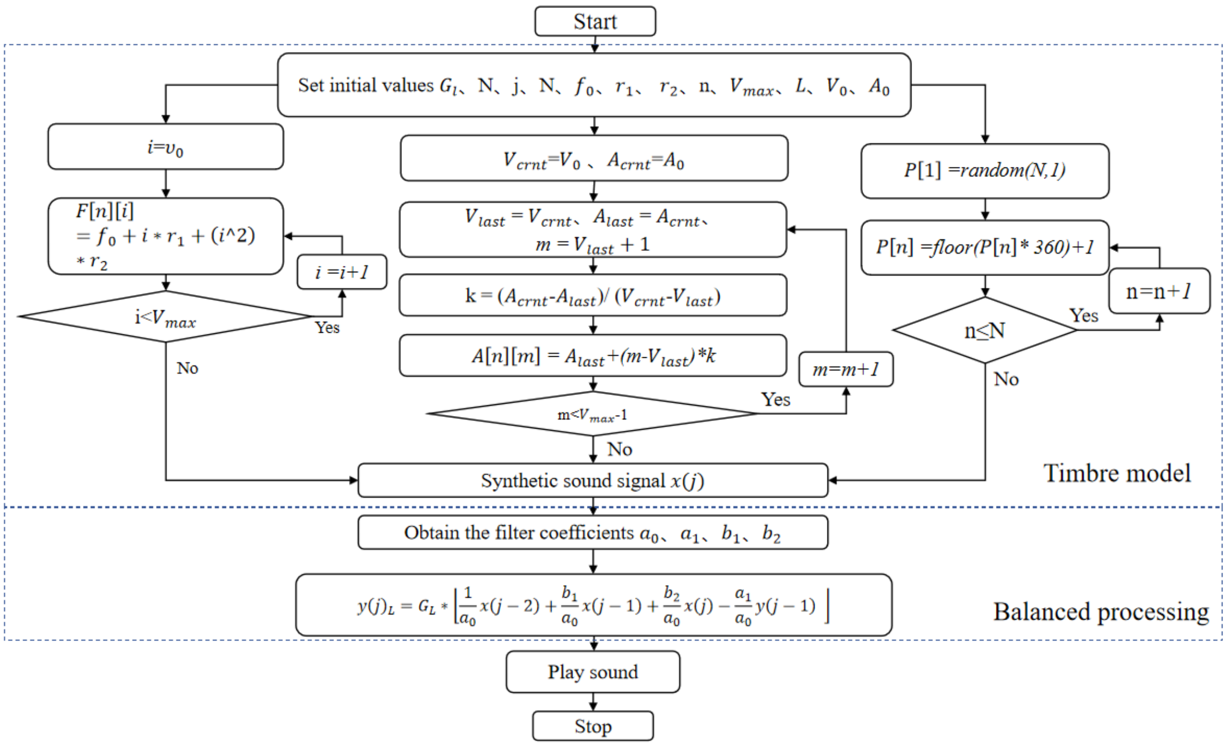

Figure 16. ASGS system algorithm flowchart.

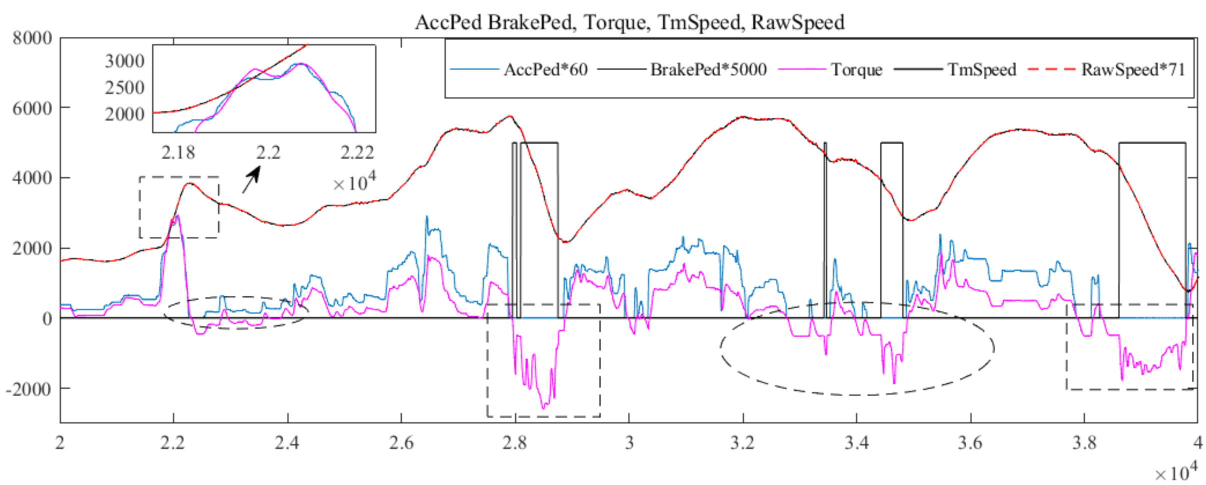

Figure 17. CAN signal.

The sound design section uses the methodology of Section 3. This article adds the overflow judgment function when acquiring the CAN signal of the vehicle, in order to improve the stability of the sound synthesis algorithm. Each time the CAN signal is read, it is full of one frame, only then is the CAN data input into the sound synthesis. When the acquired CAN signal is not full of one frame, it starts to read the data from the CAN interface. If there is a delay in the sound played by the speaker when the driver depresses the pedal, the amount of CAN data read at a time can be reduced, e.g., by delivering less than one frame of CAN data to the main sound synthesis program. The sound field equalization and timbre correction for the four positions in the vehicle were performed according to Section 4. The sound design method based on the order synthesis algorithm is shown in **Appendix Algorithm A1**. The implemented procedure, developed in Xilinx Vitis.

5. Experimental verification

5.1. Hardware system

The main chip used in the hardware system is the xczu2eg-sfvc784-2 of the Zynq UltraScale+ MPSoC series (FPGA development boards). System input signals include automotive CAN bus signals, reference microphone signals, controller audible signal sources, and human-machine interface input signals. The system output signals include the DAC-converted unamplified audible signal source as well as the human-computer interaction interface with the need to output communication signals. The system block diagram is shown in **Figure 18**. The physical diagram of the hardware system is shown in **Figure 19**. The chips used in the hardware system are listed in **Table 4**.

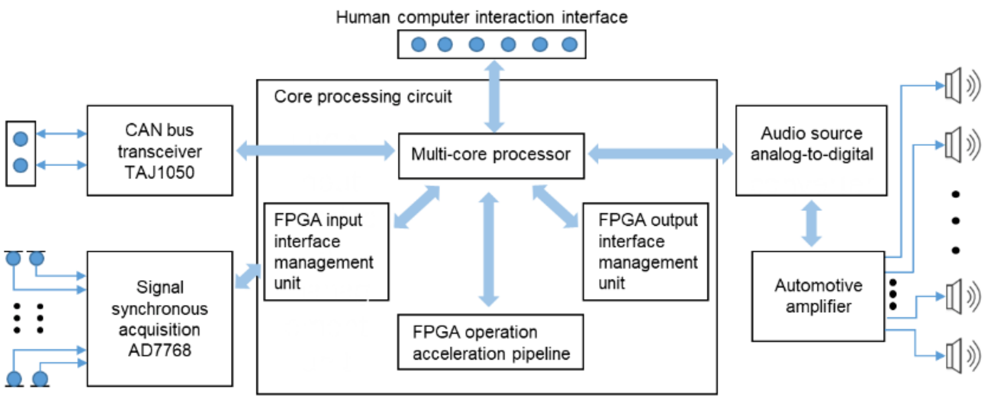

Figure 18. System schematic block diagram.

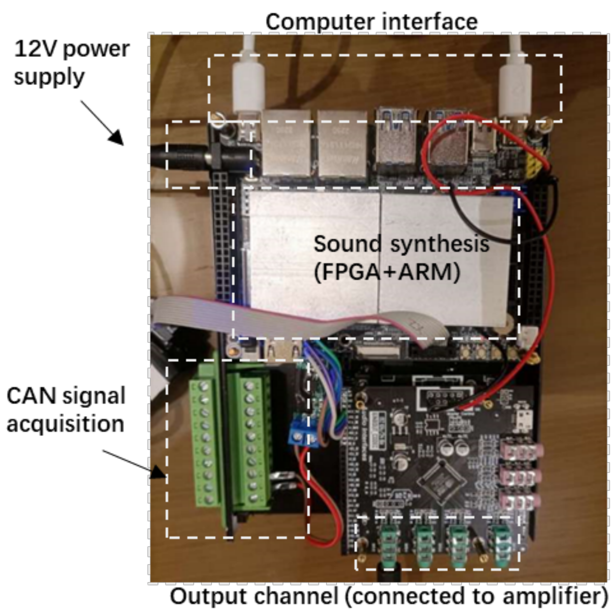

Figure 19. Hardware system.

Table 4. The chip model used in the hardware system.

Hardware module	Chip model
CAN Bus Transceiver	TJA1050 (PHILIPS)
Signal synchronous acquisition	AD7606B
Audio source analog-to-digital	LTC2755
Multi-core processor	XA7Z010
Ethernet communication	KSZ9031RNX

5.2. Experimental results

5.2.1. Objective results

The test vehicle was a tram, the basic parameters of which are shown in **Appendix A Table A2**. The road test was conducted on an ordinary road, and the test conditions were (0–120) km/h wide-open throttle (WOT) acceleration and partial throttle (POT) acceleration. The comparative graphs of the sound pressure level change with rotational speed for the two conditions are shown in **Figure 20**. The difference in sound pressure level between full-throttle and half-throttle acceleration was about 5 dB(A). The spectrum of frequency variation with rotational speed is shown in **Figure 21**. The active sound system emits sound at 600 rpm, and the test vehicle rotates up to 7,000 rpm. Considering the high motor frequency of this test vehicle, the motor sound is more obvious during driving, so the energy of the designed active sound is mainly concentrated within 1,000 Hz.

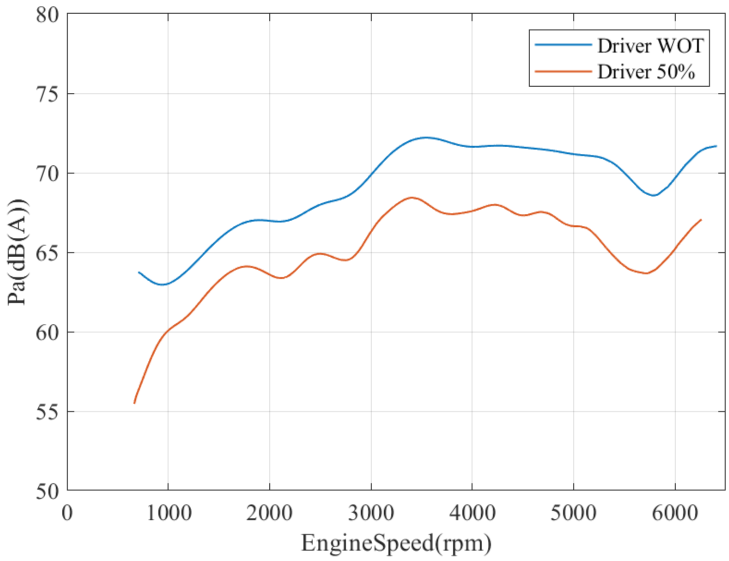

Figure 20. Comparison of sound pressure level change between WOT and POT acceleration.

The sound synthesized by the order synthesis algorithm is compared with the results of the real test conducted on the road. The road test condition is (0–120) km/h WOT acceleration, and the results of the frequency response comparison are shown in **Figure 22**. At frequencies less than 2,000 Hz, the error between the simulated data and the measured results is within 1.5 dB. At frequencies greater than 2,000 Hz, the error between the simulated data and the measured results is within 2.5 dB; in the 0–6,000 Hz band, the error rate is 5%, and the error at individual frequency points is 10%. Since there will be road noise and wind noise in the road test, the error rate between the measured and simulated data is acceptable.

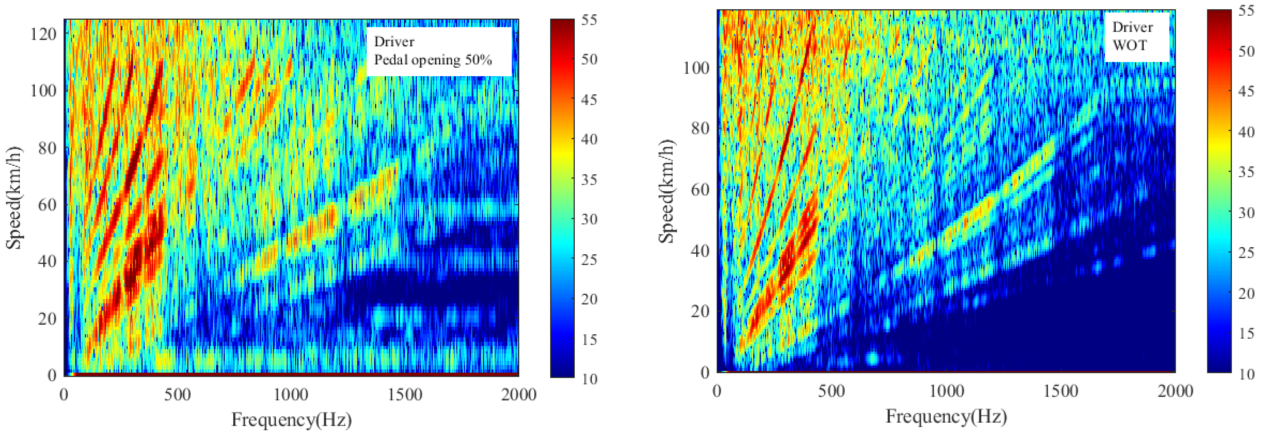

(a) Pedal opening 50%. **(b)** WOT.

Figure 21. The spectrum of frequency variation with rotational speed.

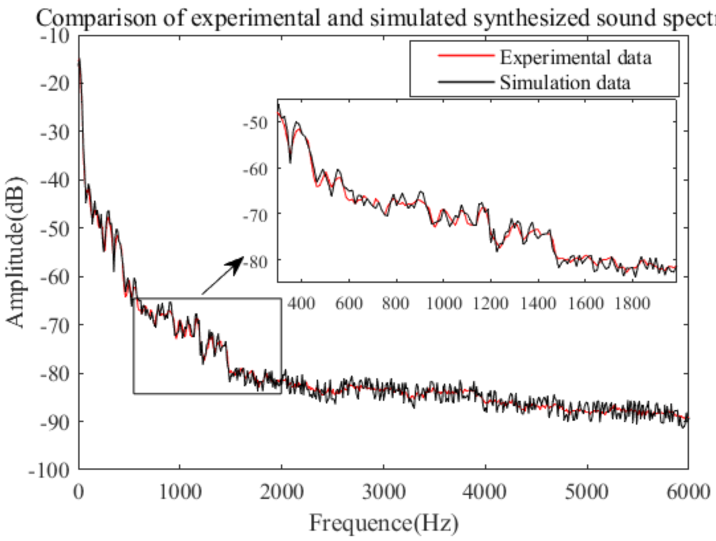

Figure 22. Comparison of frequency response between measured and simulated data.

5.2.2. Subjective evaluation

The subjective evaluation was conducted in a real vehicle, and the evaluators were free to drive on ordinary city roads.

1. Evaluation content

① Sense of motion

Positive description: Bright sound, good sound when accelerating, good dynamics at high revolutions, sound exciting.

Negative description: Low sound frequency, soft sound, lack of passion.

② Luxury feeling

Positive description: The sound pressure level of the powertrain is low, the sound characteristics of the powertrain are clear, the high-frequency sound is relatively low, the tone is pleasing to the ear, and there is a sense of comfort and luxury.

Negative description: The sound has too many high-frequency components or too many wide-frequency components, and sounds like there is a murmur, and is not refined enough.

③ Delay

Positive description: Little latency during driving, no mismatch between sound and CAN messages.

Negative description: Large latency during driving, a mismatch between sound and CAN signal changes occurs.

④ Harmony

Positive description: The sound sounds pleasant and blended, and the sound has no sudden changes or discordant components.

Negative description: The sound has sudden changes and discordant components.

2. Subjective evaluation rating scale

The subjective evaluation scale is shown in **Table 5**. Different scores correspond to different levels of perception and satisfaction.

Table 5. Subjective evaluation rating scale [35,36].

Score	1	2	3	4	5	6	7	8	9	10
Performance evaluation	unacceptable		Very poor		edge	Acceptable	commonly	good	very nice	fantastic
Satisfaction	Very dissatisfied				Slightly dissatisfied	Basically satisfied		Very satisfied	Very satisfied	

3. Subjective evaluation scoring

Fifteen personnel participated in the subjective evaluation, and the evaluation scores are shown in **Table 6**. The basic information of the fifteen participants is shown in **Table 7**.

Table 6. Subjective evaluation scoring.

Evaluators	Sense of motion score (1–10)	Luxury feeling score (1–10)	Delay score (1–10)	Harmony score (1–10)	Composite score (1–10)
1	7.25	6.5	9	8	7.7
2	7.5	7	8	7.75	7.6
3	8	7.5	8.5	7.75	7.9
4	7.75	8	8	8	7.9
5	7.75	7	8.5	8.25	7.9
6	8	7.5	8.25	8	7.9
7	8.25	7.5	8.5	8.25	8.1
8	8.5	8.25	9	8.25	8.5
9	8.25	8.5	8.5	7.75	8.3
10	8	7.5	8.75	8.5	8.2
11	8.25	7.75	9	7.25	8.1
12	7.75	7.25	8.75	7.5	7.8
13	8.5	8.25	9	8.5	8.6
14	8	8	7.5	8.25	7.9
15	8.25	6.5	8.75	8	7.9
Average	8	7.5	8.5	8	8

Table 7. The basic information of the fifteen participants.

Occupation	Age	Gender
Four NVH designers, four marketing and sales personnel, four CAE designers, and three decision-makers.	Five individuals under the age of thirty, eight individuals between thirty and forty, and two individuals over the age of fifty.	Ten men and five women.

6. Conclusion

The main proposal of this article presents a sound synthesis algorithm based on order synthesis and IIR filters for designing multi-style sound waves. The main work is as follows:

1. Sound style flexible design: Establish amplitude gain control and frequency gain control mechanisms for dynamic parameters such as speed and torque, and develop timbre models based on linear interpolation. The flexible model definition approach enables the design of diverse sound styles.
2. Sound field equalization and timbre correction: Based on the IIR filter, the sound field equalization and timbre correction are carried out at the four measurement points in the vehicle, and the sound pressure level error of the four measurement points after the equalization is within 3 dB(A). Reduce auditory differences between the four seats in the vehicle.
3. Real vehicle robustness verification: The hardware system built on ARM and FPGA was integrated into the tram for real-vehicle debugging. Comparing real-vehicle and simulated data, the error rate in the 0–6,000 Hz frequency band was 5%, with a single frequency point error of 10%. Subjective evaluation of the sound was conducted based on four dimensions (sense of motion, sense of luxury, latency, and harmony), yielding a subjective evaluation score of 8 points.

Future research will focus on optimizing control strategies for sound synthesis and investigating the impact of phase on sound quality, thereby enhancing audio fidelity to meet diverse market demands. Additionally, hardware devices will be optimized to improve real-time performance and scalability. To adjust the balance of a vehicle during operation, it is necessary to incorporate a virtual microphone to obtain feedback signals for real-time adjustments.

Author contributions: Conceptualization, XZ and JD; methodology, XZ and JB; formal analysis, HL; software programming, SW and CL; testing and validation, HL and CZ; writing and supervision, XZ and JD. All authors have read and agreed to the published version of the manuscript.

Funding: This work was not supported by any funding.

Institutional review board statement: Not applicable.

Informed consent statement: Not applicable.

Data availability statement: The data that support the findings of this study are available from the corresponding authors upon reasonable request.

Conflict of interest: The authors declare no conflicts of interest.

AI use statement: The authors declare that no artificial intelligence (AI) tools were used in the preparation of this manuscript.

References

1. Lanslots J, Bodden M, Macdonald S, et al., Comprehensive Automotive Active Sound Design. In: Proceedings of the 2020 National Conference on Noise Control Engineering; 16–18 November 2020; New Orleans, LA, USA. Available online: https://www.product-sound.de/assets/images/NC20_459.pdf
2. Falchi S. Engine Sound Enhancement and Customization Based on Granular Synthesis [Master's Thesis]. Politecnico di Torino; 2020. Available online: https://webthesis.biblio.polito.it/16002/1/tesi.pdf
3. Petersen M, Deml B, Albers A. The Effect of an Emotionalizing Sound Design on the Driver's Choice of Headway in a Driving Simulator. Acoustics. 2024; 6(2): 541–567. doi: 10.3390/acoustics6020029
4. Yeoh JPS, Han MG, Spence C. The Impact of Musical Fit and Sound Design on Consumers' Perception of a Luxury Car Ad. Luxury. 2022; 9(2–3): 165–184. doi: 10.1080/20511817.2022.2224496
5. Bodden M, Belschner T. Legal requirements and design of exterior sounds for electric vehicles. In: Internationales Stuttgarter Symposium. Springer; 2018. pp. 969–980. doi: 10.1007/978-3-658-21194-3_73
6. Jagla J, Maillard J, Martin N. Sample-based engine noise synthesis using an enhanced pitch-synchronous overlap-and-add method. The Journal of the Acoustical Society of America. 2012; 132(5): 3098–3108. doi: 10.1121/1.4754663
7. Balger A, Lanslots J, Bodden M. Active Sound Design : Abwägung zwischen Gestaltungsfreiheit und Ressourcenanforderung = Active Sound Design : Trade-off between freedom of design and required resources. Otto von Guericke University Library; 2023. doi: 10.25673/103521
8. Amman SA, Das M. An efficient technique for modeling and synthesis of automotive engine sounds. IEEE Transactions on Industrial Electronics. 2001; 48(1): 225–234. doi: 10.1109/41.904583
9. Xenakis I, Formalized Music. Indiana University Press; 1971.
10. Roads S, Strawn JM. Foundations of Computer Music. MIT Press; 1987.
11. Chen F, Zhang X. Synthesising the sound of a car engine based on envelope decomposition and overlap smoothing. Journal of Vibroengineering. 2021; 23(5): 1254–1266. doi: 10.21595/jve.2021.21920
12. Moulines E, Charpentier F. Pitch-synchronous waveform processing techniques for text-to-speech synthesis using diphones. Speech Communication. 1990; 9(5–6): 453–467. doi: 10.1016/0167-6393(90)90021-Z
13. Verhelst W, Roelands M. An overlap-add technique based on waveform similarity (WSOLA) for high quality time-scale modification of speech. In: Proceedings of the IEEE International Conference on Acoustics Speech and Signal Processing; 27–30 April 1993; Minneapolis, MN, USA. pp. 554–557. doi: 10.1109/ICASSP.1993.319366
14. Lazaro MJ, Kim S, Choi M, et al. Design and Evaluation of Electric Vehicle Sound Using Granular Synthesis. Journal of the Audio Engineering Society. 2022; 70(4): 294–304. doi: 10.17743/jaes.2021.0062
15. Xie L, Lu C, Liu Z, et al. A method of generating car sounds based on granular synthesis algorithm. Noise Control Engineering Journal. 2022; 70(4): 384–393. doi: 10.3397/1/377031
16. Yu S, Xie L, Lu C, et al. Research on Design of Electric Vehicle Sound Synthesis Based on Frequency Shift Algorithm. In: Proceedings of the WCX SAE World Congress Experience; 9 April 2024; Detroit, MI, USA. doi: 10.4271/2024-01-2335
17. Chang KJ, Kim S, Park DC, et al. A Research on Brand Sound Positioning and Implementing with Active Sound Design. In: Proceedings of the Noise and Vibration Conference and Exhibition, Grand Rapids; 5 June 2017; Grand Rapids, MI, USA. doi: 10.4271/2017-01-1754
18. Blake A. Game Sound, An Introduction to the History, Theory, and Practice of Video Game Music and Sound Design. Journal of Design History. 2009; 22(3): 294–295. doi: 10.1093/jdh/epp021
19. Heitbrink DA, Cable S. Design of a driving simulation sound engine. In: Proceedings of the 2007 Driving Simulation Conference (DSCNA 2007); 12–14 September 2007; Iowa City, IA, USA. Available online: https://www.nads-sc.uiowa.edu/bio_pub_pdf/Heitbrink_&_Cable_-_Design_of_a_driving_simulation_sound_engine.pdf
20. Farnell A. Behaviour, Structure and Causality in Procedural Audio. In: Game Sound Technology and Player Interaction: Concepts and Developments. IGI Global; 2011. pp. 313–339. Available online: https://www.igi-global.com/gateway/chapter/46798
21. Bodden M, Belschner T. Consistent Active Sound Generation Concept for Hybrid vehicles. In: Proceedings of the 48th International Congress and Exposition on Noise Control Engineering (INTERNOISE 2019); 16–19 June 2019; Madrid, Spain. pp. 6869–6878.
22. Bodden M, Belschner T. Comprehensive Active Sound Design. Part 1: Electric and combustion vehicles. In:

Proceedings of the 43rd International Congress on Noise Control Engineering (INTERNOISE 2014); 16–19 November 2014; Melbourne, VIC, Australia. Available online: https://acoustics.asn.au/conference_proceedings/INTERNOISE2014/papers/p467.pdf
23. Belschner T, Bodden M. Comprehensive Active Sound Design. Part 2: Operational sounds and Brand Sound. In: Proceedings of the 43rd International Congress on Noise Control Engineering (INTERNOISE 2014); 16–19 November 2014; Melbourne, VIC, Australia. Available online: https://acoustics.asn.au/conference_proceedings/INTERNOISE2014/papers/p469.pdf
24. Sontacchi A, Frank M, Höldrich R. In-car Active Sound Generation for enhanced feedback in vehicles with combustion engines or electric engines. In: Proceedings of the Workshop on In-Vehicle Auditory Interactions at the 21st International Conference on Auditory Display (ICAD-2015); 6 July 2015; Graz, Austria. Available online: https://www.researchgate.net/publication/279837871_In-car_Active_Sound_Generation_for_enhanced_feedback_in_vehicles_with_combustion_engines_or_electric_engines
25. Zhang S, Li Y, Xu L, et al. Development of an Active Sound Generation System for Sound Quality in EVs at Constant Speed Combined with Subjective Evaluation. Applied Sciences. 2022; 12(21): 10768. doi: 10.3390/app122110768
26. Zhang S, Li Y, Cao Y, et al. Research on active sound control in EV in-vehicle based on engine order sound fitting. Advances in Mechanical Engineering. 2023; 15(6). doi: 10.1177/16878132231181282
27. Zhang S, Li Y, Jiang H, et al. Research on the characteristics of EV interior sound quality and its dynamic active control system design and development under accelerated driving conditions. PLOS ONE. 2024; 19(4): e0290150. doi: 10.1371/journal.pone.0290150
28. Fu J, Zhu C, Su J. Research on the Design Method of Pure Electric Vehicle Acceleration Motion Sense Sound Simulation System. Applied Sciences. 2022; 13(1): 147. doi: 10.3390/app13010147
29. Chang KJ, Park DC. Technology of an Emotional Engine Sound Designing for Active Sound Control Using Order Balance and Musical Instrument Sound. In: Proceedings of the 9th International Styrian Noise, Vibration & Harshness Congress: The European Automotive Noise Conference; 15 June 2016; Graz, Austria. doi: 10.4271/2016-01-1782
30. Min D, Park B, Park J. Artificial Engine Sound Synthesis Method for Modification of the Acoustic Characteristics of Electric Vehicles. Shock and Vibration. 2018; 2018(1): 5209207. doi: 10.1155/2018/5209207
31. Litwin L. FIR and IIR digital filters. IEEE Potentials. 2000; 19(4): 28–31. doi: 10.1109/45.877863
32. Stainsby T, Cross I. The Perception of Pitch. Oxford University Press; 2012. doi: 10.1093/oxfordhb/9780199298457.013.0005
33. Andersen TH, Jensen KK. Phase Modeling of Instrument Sounds Based on Psycho Acoustic Experiments. In: Proceedings of the Workshop on current research directions in computer music; 15–17 November 2001; Barcelona, Spain. Available online: https://www.researchgate.net/publication/2486450_Phase_Modeling_of_Instrument_Sounds_Based_on_Psycho_Acoustic_Experiments
34. Plomp R, Steeneken HJM. Effect of Phase on the Timbre of Complex Tones. The Journal of the Acoustical Society of America. 1969; 46(2B): 409–421. doi: 10.1121/1.1911705
35. Zhang S, He FF, Xu W, et al. Study on Active Control and Evaluation Methods for In-Vehicle Sound Quality of EV Under Driving at a Constant Speed. International Journal of Automotive Technology. 2025; 26(4): 1045–1065. doi: 10.1007/s12239-025-00209-9
36. Zhang S, Li Y, Jiang H, et al. Research on the parameter design and calibration and control of EV in-vehicle active sound generation system. Heliyon. 2024; 10(7): e27407. doi: 10.1016/j.heliyon.2024.e27407

Appendix A

Table A1. Parameter meaning table.

G_l	Gain for each speaker
N	Total Order Number
f_0	Initial frequency
r_1	Coefficient of the linear velocity in frequency calculations
r_2	Coefficient of the quadratic term for velocity in frequency calculation
n	The numerical value of the current order
V_{max}	Maximum speed
A_0	Initial amplitude

Table A1. *Cont.*

V_0	Initial speed
V_{crnt}	Speed of the current frame
A_{crnt}	Amplitude of the current frame
V_{last}	Speed of the previous frame
A_{last}	Amplitude of the previous frame
k	Frame-by-frame amplitude variation rate
P $[n]$	Phase of the n-th order
A [n] $[i]$	The magnitude of the n-th order at velocity i
F [n] $[i]$	The frequency of the n-th order at velocity i
X $[j]$	Synthetic sound signal
Y $[j]_l$	The audio signal emitted by each speaker after equalisation processing
L	Number of speakers
a_0, a_1, b_0, b_1	Filter coefficients
j	Data volume per frame

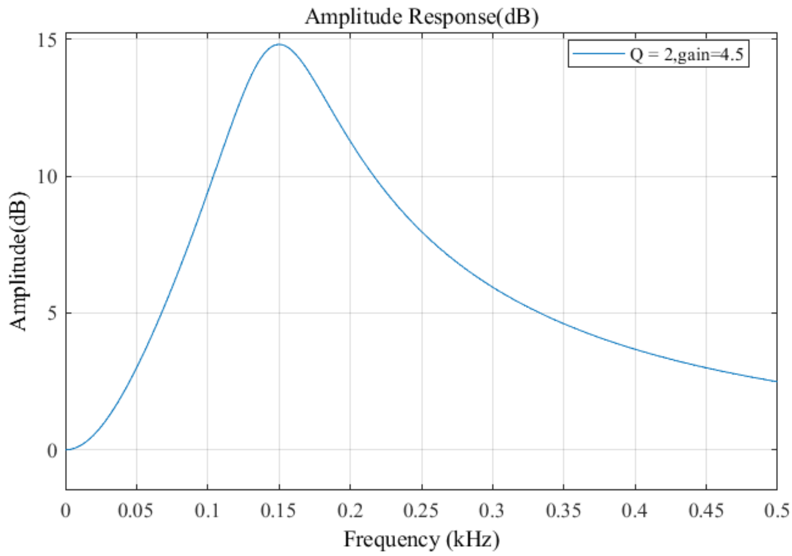

Figure A1. IIR peak filter diagram.

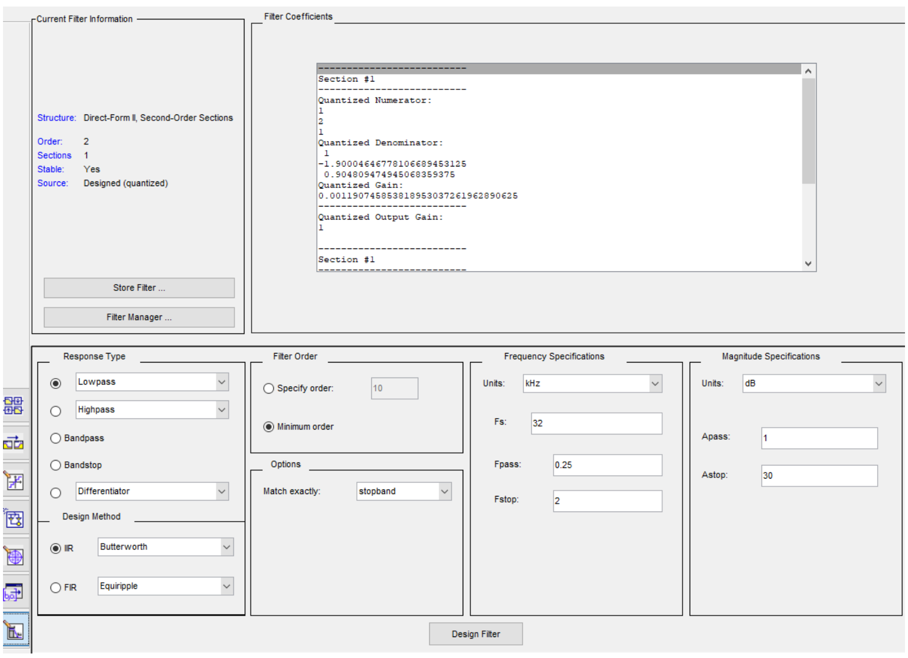

Figure A2. Butterworth filter for 0–250 Hz.

Algorithm A1 Order Synthesis Algorithm

Input: Vehicle CAN signal.

Output: Algorithmic synthesis of sound.

Interrupt initialize
CAN initialize
Sound output channel initialization
Sound Produce initialize
Initialization of sound design section
Equalize Instance
Start the main function
define HarmNum=[] and Gain_A=[] and Gain_B=[] and Gain_C=[] and Gain_D=[]
Data written into sound channel, write 0 blocks and 960 sampling points per block.
Can signal processing and transmitting data to the sound design section
While (runfag)
    for $(i = 0;\ i < 1;\ i{+}{+})$ **then**
        if $(j = 0;\ j < NumPoints\,;\ j{+}{+})$
            $Genout[j] = Ampl_{crnt}$
            $Freq_{crnt} = Freq_{crnt} + Freqstep$
        end if
    for $(l = 0;\ l < HarmNum\,;\ l{+}{+})$**do**
        $Freq_{start}[l] = Freq_{end}[l]$
        $Freq_{end}[l] = FreqMode[l][Speed_{crnt}]$
        $Ampl_{end}[l] = AmplMode[l][Speed_{crnt}]$
        if $(Torq_{crnt} < 0)$**then**
            $Ampl_{end}[l] = (a_1 + a_2 * Torq_{crnt}) * Freq_{end}[l]$
        else
            $Ampl_{end}[l] = (a_3 + a_4 * Torq_{crnt}) * Freq_{end}[l]$
        end if
        $Freq_{crnt} = Freq_{start}[idxharm]$
        $Freqstep = (Freq_{end}[idxharm] - Freq_{start}[idxharm])/NumPoints$
        $Ampl_{crnt} = Ampl_{start}[idxharm]$
        $Amplstep = (Ampl_{end}[idxharm] - Ampl_{start}[idxharm])/NumPoints$
        $SndGenOut = GenOut[i]$
    end for
    Run the balancing algorithm
end for
for $(i = 0;\ i < NumPoints\,;\ i{+}{+})$ **do**
    $DataCh_n = EqualData_n * Gain_n$
end for
while $(CanBuffer == 0)$ **do**
    if $(RxFrame[0] == (u32)XCanPs\_CreateIdValue((u32)0x[][])$ **then**
        $EffectValue = (u32)(RxFrame[2])$
        $Torq = EffectValue$

```
            TorqBias += 1
              if (TorqBias >= 100) then
            TorqBias = 0
            end if
            TorqWholeCrnt = EffectValue
            GetTorq = 1
          end if
        Obtain information such as vehicle speed, motor speed, pedal opening, etc.
        if (SnyData < 0) then
            return -1
        else if (SynData < Single − frame data) then
              return 1
        else
            return -2
        end if
    end while
    Play sound
```

Table A2. Basic parameters of the test vehicle.

Type of energy	Electric vehicle
Maximum power (kW)	405
Maximum torque (N·m)	750
Number of drive motors	Dual Motor
Front motor model	CAM220PT2
Rear motor model	CAM250PT1
Motor type	Permanent magnet/synchronous